# Proposed active control methodologies for aeolian vibration of suspended cables under icing conditions

Yiqing Meng[1], Laszlo E. Kollar[1]

[1] *Savaria Institute of Technology*
*ELTE Eötvös Loránd University, Budapest, Hungary*

my@inf.elte.hu, kl@inf.elte.hu

*Abstract*— **The main objective of the research described in this paper is to propose two active vibration control techniques for eliminating aeolian vibration problems of suspended cables. It is also aimed to extend the applicability of the technique under icing conditions. These problems are commonly encountered in such applications as power transmission lines and cable-supported bridges. Limited research has previously been done into the use of active vibration control for attenuating the vibration amplitude of suspended cables, especially under icing conditions. This paper describes the development of an Electrical Vibration Absorber (EVA) capable of reducing the vibration amplitude in aeolian vibration of a single cable. The suspended cable and the proposed electrical vibration absorber are modelled using SIMULINK software. The first proposed control methodology involving the use of PID has been implemented enabling the value of the cable displacement and acceleration to be significantly reduced when the aeolian vibration occurred, compared to the conventional vibration absorber. The extensive control methodology of EVA system has also been proposed based on estimation of cable vibration frequency to determine the dynamic performance of the controller. The simulation results of extensive control methodology demonstrate that the amplitude of vibration is smaller than that with the use of passive vibration absorber.**

Keywords— ***aeolian vibration, active vibration control, electrical vibration absorber, PID control, frequency estimation***

## I. INTRODUCTION

Cable structures have become increasingly important over the last decades in variety of engineering applications, such as the cable-supported bridges and power transmission lines. However, there is a well-marked problem on improving the safety of suspended cable-based structures due to the fact that cables are exposed to wind induced vibration. The effects of wind are especially noticeable in cold climate regions where atmospheric ice accumulates frequently on the cable resulting in D- or U-shaped cross-sections, which is linked to an increased risk of fatigue failure of the cable. One of the significant sources of damage is the high-speed vortex shedding excitation, the so-called 'aeolian vibration' [1, 2]. In practice, the amplitude of the aeolian vibration is relatively small, i.e. similar to the cable diameter. The frequency of this vibration is usually in the range of 3 Hz to 150 Hz for wind speed of 1-10m/s [3, 4]. In order to overcome this issue, a number of technologies have been invented and developed. Torsional dampers were applied for transmission lines and effectively reduced the amplitude of aeolian vibration; however, torsional dampers operate in a limited frequency range and are deactivated during the winter [5]. An alternative technique, the application of the so-called Elgra dampers is able to give frequency response in a relatively large range, based on the movable three cast masses, but this device is noisy and has additional abrasions at the junction on the cable [1]. Another well-known device, the Stockbridge-type damper, is designed to dissipate vibration energy by moving two end-masses with multiple resonant frequencies, which can be effective over a wide range of aeolian vibration frequency. The excessive wear of the messenger cable means a particular limitation for this type of technique even though these devices have widely been used in different cable structures [1, 6]. More recently, semi-active-type vibration control techniques, like the application of Magnetorheological (MR) dampers, are developed and implemented in cable-supported bridges due to their large adjustable damping force and quick response [7, 8]. Nevertheless, the physical system of this technique was designed to be near the ground close to the cable lower end. This means that the cable vibration cannot be fully controlled. Additionally, the calibration and maintainability are considered to be the major limitations of this technique due to the relatively complicated calibration procedures and to the fact that the parameters obtained in the laboratory calibration may not be valid for realistic application [1, 8-12]. In the present paper, a novel active vibration controller, the so-called Electrical Vibration Absorber (EVA) system, is proposed in order to suppress and prevent cable vibration. The proposed EVA system has no limitation on installation, which means that it can be used at any location along the cable. On the other hand, by continuously providing the control force, the EVA system is effective in a relatively wide frequency range.

## II. SYSTEM DESCRIPTION AND MATHEMATICAL MODEL

### A. Dynamic model of cable-EVA system

The vibration absorber (VA) is a classical device to transfer the vibration energy from a primary structure to a secondary mass. If the natural frequency of the absorber is toned to the natural frequency of the primary structure then the amplitude of vibration will be strikingly attenuated. Based on this characteristic, the electrical actuator-based vibration controller has been selected for use with VA for EVA system in the present research. The 2-degree-of-freedom (2-DOF) model of EVA system in a suspended cable is shown in Fig.1, where the mass of the cable (or ice loaded cable) and that of the EVA system are represented by $m_1$ and $m_2$, respectively; $k_1$ denotes the elasticity of the cable in the vertical direction, $c_1$ describes the structural damping of the cable; $k_2$ and $c_2$ are the spring stiffness and damping ratio of the EVA,

respectively, and $x_1$ and $x_2$ denote the vertical displacements of $m_1$ and $m_2$, respectively.

It can be seen in Fig.1 that, when the wind force $F(t)$ acts on the cable, the control force $f_c$ is generated and works on both objectives. The vibration of cable will be cancelled out if the control force $f_c$ is exactly identical in magnitude but reverse in phase to $F(t)$. It is worth noting that, for this study, the spring $k_2$ and damping $c_2$ are not used for the control, so the value of $k_2$ and $c_2$ are chosen to consider the elasticity and structural damping of the device.

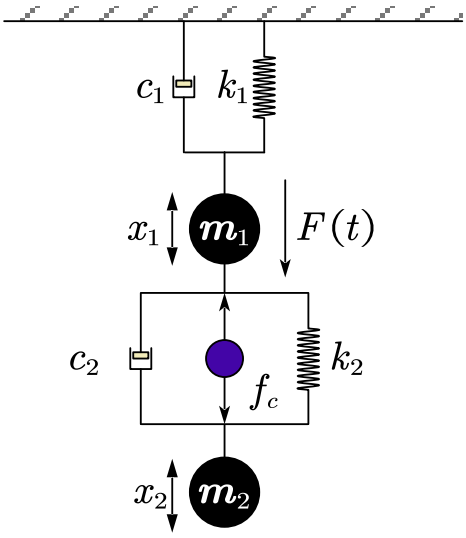


Fig.1 The 2-DOF model of EVA system in a suspended cable

By employing the free-body diagram and Newton's 2nd law of motion, the governing equation of the cable-EVA system (see Fig.1) can be written as follows:

$$M\ddot{X} + C\dot{X} + KX = Q \tag{1}$$

where

$$M = \begin{bmatrix} m_1 & 0 \\ 0 & m_2 \end{bmatrix} \qquad C = \begin{bmatrix} c_1 + c_2 & -c_2 \\ -c_2 & c_2 \end{bmatrix} \qquad K = \begin{bmatrix} k_1 + k_2 & -k_2 \\ -k_2 & k_2 \end{bmatrix}$$

$$X = \begin{bmatrix} x_1 \\ x_2 \end{bmatrix}$$

$$Q = \begin{bmatrix} F(t) - f_c \\ f_c \end{bmatrix}$$

The dynamic motion of the cable-EVA system can be expressed as a state-space model in the form:

$$\dot{\bar{X}} = A\bar{X} + BU \tag{2}$$

$$Y = E\bar{X} \tag{3}$$

where

$$\dot{\bar{X}} = \begin{bmatrix} \dot{x}_1 \\ \ddot{x}_1 \\ \dot{x}_2 \\ \ddot{x}_2 \end{bmatrix} \quad A = \begin{bmatrix} 0 & 1 & 0 & 0 \\ -\frac{k_1 + k_2}{m_1} & -\frac{c_1 + c_2}{m_1} & \frac{k_2}{m_2} & \frac{c_2}{m_1} \\ 0 & 0 & 0 & 1 \\ \frac{k_2}{m_2} & \frac{c_2}{m_2} & -\frac{k_2}{m_2} & -\frac{c_2}{m_2} \end{bmatrix} \quad \bar{X} = \begin{bmatrix} x_1 \\ \dot{x}_1 \\ x_2 \\ \dot{x}_2 \end{bmatrix}$$

$$B = \begin{bmatrix} 0 & 0 \\ \frac{1}{m_1} & -\frac{1}{m_1} \\ 0 & 0 \\ 0 & \frac{1}{m_2} \end{bmatrix} \quad U = \begin{bmatrix} F(t) \\ f_c \end{bmatrix} \quad E = [1 \;\; 0 \;\; 0 \;\; 0]$$

There are several parameters in the model, e.g. the spring stiffness of cable $k_1$, that must be defined before developing the control system. The detailed discussion for determining these parameters can be found in previous research on the iced-cable vibration by [13] who proposed a mathematical model to express dynamic effects of vibration on a twin bundle with a spacer induced by ice shedding. The definitions of parameters used in this study are shown below.

The mass of cable loaded by ice, $m_1$, can be written as shown by Eq (4):

$$\begin{aligned} m_1 &= \left[\mu + \rho_{ice}\frac{(D_c + 2b_{ice})^2 - D_c^2}{4}\pi\right]L_c \quad \text{(circular shape ice)} \\ m_1 &= \left[\mu + \rho_{ice}\frac{(D_c + 2b_{ice})^2 - D_c^2}{8}\pi\right]L_c \quad \text{(D shape ice)} \end{aligned} \tag{4}$$

where $\mu$ is mass per unit length, $\rho_{ice}$ is density of ice, $D_c$ is diameter of bare cable, $b_{ice}$ is thickness of ice, and $L_c$ is the span length.

A review of previous research [13] indicates that the spring stiffness of the iced cable is calculated in two steps. Firstly, the horizontal tension of the iced cable should be obtained. This calculation can be done by using the following equation[13, 14]

$$h_d^3 + \left(2 + \frac{\lambda^2}{24}\right)Hh_d^2 + \left(1 + \frac{\lambda^2}{12}\right)H^2h_d - \frac{\lambda^2}{12}\frac{pH^3}{\mu g}\left(1 + \frac{p}{2\mu g}\right) = 0 \tag{5}$$

where $H$ and $h_d$ represent the initial tension of the bare cable and the additional tension due to ice load, respectively. The term $\lambda^2$ may be calculated as follows

$$\lambda^2 = \frac{(\mu g L_c)^2}{H}\frac{EA}{HL_e} \tag{6}$$

The next step is to determine the displacement of iced-cable in the position where the EVA system is placed. For this purpose, the relationship between the vertical force, $P_z$, and the resultant vertical displacement, $w_p$, is investigated, and it may be described as follows

$$w_p(x) = \frac{P_z L_c}{\tilde{H} + h_{pz}}\left[\left(1 - \frac{x_p}{L_c}\right)\frac{x}{L_c} - \frac{h_{pz}mgL_c}{2\tilde{H}P_z}\frac{x}{L_c}\left(1 - \frac{x}{L_c}\right)\right] \tag{7}$$

where the additional tension, $h_{pz}$, due to the concentrated load, acting from the EVA system in the case considered, is given by

$$h_{pz}^3+\left(2+\frac{\tilde{\lambda}^2}{24}\right)\tilde{H}h_{pz}^2+\left(1+\frac{\tilde{\lambda}^2}{12}\right)\tilde{H}^2h_{pz}-\tilde{\lambda}^2\frac{P_z\tilde{H}^3}{2\mu gL_c}\left(1+\frac{P_z}{\mu gL_c}\right)\bullet\left(\frac{x_p}{L_c}-\frac{x_p^2}{L_c^2}\right)=0 \tag{8}$$

with $\tilde{H}=H+h_d$ $\tilde{\mu}=m_1$ and $\tilde{\lambda}^2=\left(\mu gL_c/\tilde{H}\right)^2/\left(\tilde{H}L_e/EA\right)$

Once the results are obtained by using the above equations, an appropriate polynomial function is fitted to the $w_p$ versus $P_z$ relationship. Since the amplitude of aeolian vibration is not greater than 2-3 times the displacement of cable, this relationship can be considered linear. Thus, it can be expressed in the form $P_z=k_1w_p$.

### *B. Actuator model*

Carefully choosing the type of actuator is essentially important, because this choice has a significant effect on the reliability of the EVA. The properly chosen actuator cannot only generate sufficiently large control force applied to the cable, but it also has relatively fast time response. A non-commutated DC linear actuator has been selected in the present study for using with the electrical driving circuit for the EVA. The control force provided with this actuator is only proportional to the coil current in the permanent magnetic field, which makes the system easy to troubleshoot and maintain. Another benefit of using this actuator is that it can produce a constant force over the stroke. The dynamic behaviour of the actuator is described by a first order system. The differential equation of the actuator is written in the form

$$f_c=Gi(t) \tag{9}$$

$$L\frac{di(t)}{dt}+Ri(t)=V(t) \tag{10}$$

where *G* represents constant gain value, $i(t)$ is the current of the coil, *L* and *R* denote the inductance and resistance of the coil, respectively, and the *V(t)* is the control voltage signal. Thus, Eqs (9) and (10) can be expressed as a state-space model in the form

$$\dot{X}_c=-\frac{RG}{L}X_c+\frac{G}{L}V(t)$$
$$Y_c=X_c \tag{11}$$

where $\dot{X}_c=\dot{f}_c$ , $X_c=f_c$.

### *C. Mechanical design of EVA system*

After the theoretical background of cable-EVA system has been investigated, it should be studied how to relate the 2-DOF model to the practical design in order to satisfy the application requirements. Fig.2 (a) and (b) present the scheme and a CAD drawing of the EVA system, respectively. By inspection of Fig.2 (a), it can be seen that the EVA consists of the actuator, accelerometer, helical spring, EVA cover and cable holder.

The EVA cover shown in Fig.2 (b) consists of two sections that can be easily assembled (or disassembled) through two M2 screws. This design facilitates the replacement if any section is damaged. The cylindrical grooves on the bottom section have been designed to hold the stator of the actuator and the coil holder which form the common linear voice coil actuator configuration. It is worth noting that the body of EVA is constructed from ferromagnetic material because its relative permeabilities will not affect the magnetic flux density distribution in the actuator. The helical spring was designed to bear the weight of EVA and to keep sufficient space between the cable and the EVA cover. Another benefit of this design is that the EVA is turned to be a conventional vibration absorber when the actuator is disabled, which can be considered as a fail-safe device.

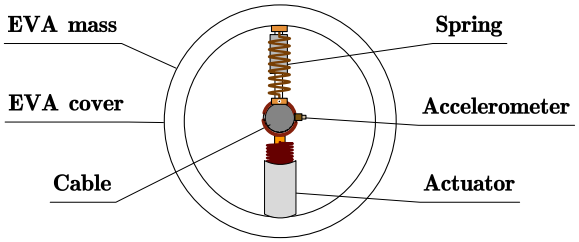


(a)

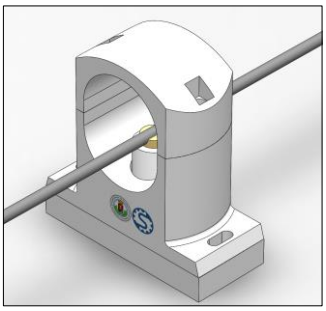

(b)

Fig.2 The EVA system (a) schematic diagram (b) CAD drawing

## III. CONTROL METHODOLOGIES

### *A. PID control methodology*

The first control methodology applied with the EVA system is based on the conventional PID control. The reason for selecting this method is that the PID controller is by far the most popular and robust algorithm for active design of civil structures. Another reason for this choice is that the use of PID controller is helpful for understanding and thus improving the design of EVA system due to fact that the gains can be manipulated. The general form of a PID controller is written as follows

$$V(t)=K_pe(t)+K_i\int_0^t e(\tau)d\tau+K_d\frac{d}{dt}e(t) \tag{12}$$

The control signal $V(t)$ is defined as the sum of three terms: proportional, integral and differential. The proportional term can generate control output by multiplying the current error *e*(*t*) (i.e. vibration amplitude in the present study) with adjustable gain $K_p$. The contribution from the integral term is to eliminate the steady state error by multiplying the gain $K_i$ with the sum of the instantaneous error over time. The derivative term predicts the system behaviour and compensates the control signal by multiplying the velocity of vibration with the gain $K_d$.

However, there are some practical issues that must be considered when implementing the PID in the EVA system. They are summarized in the following.

*1) Derivative filtering:* Fig.3 illustrates the flow chart for implementing the PID strategy for the cable-EVA system. The PID strategy was implemented based on a feedback control, where the displacement signal was measured by the accelerometer and then fed back to the input to form an error signal that will be the input signal of the PID controller. In the case when a small high frequency noise is present in the output signal of the accelerometer, the accuracy of the control signal will be significantly influenced by the noise. Therefore, a first order low pass filter with cut-off at a frequency of *N* rad/s was applied into the differential term in order to remove the high frequency components. The resultant PID controller used in this study may be written in following form:

$$H_{PID}(s) = K_p + K_i \frac{1}{s} + K_d \frac{N}{1 + \frac{N}{s}} \tag{13}$$

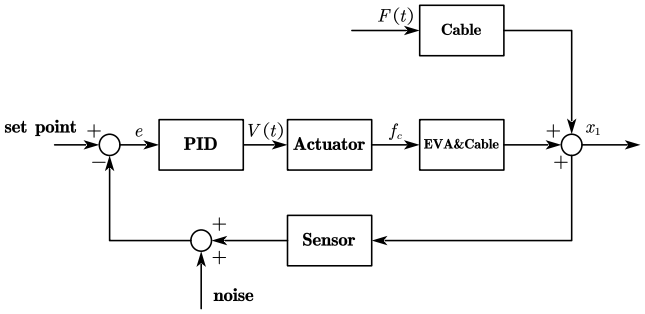


Fig.3 Block diagram of the closed-loop PID control system for iced-cable vibration

2) *Integrator clamping:* As mentioned earlier, the integral term is used to improve the accuracy of the control signal by eliminating the steady state error. However, when the actuator is not able to follow the control command due to its limitations, the integral term likely leads to controller saturation. Consequently, even when the vibration amplitude attains the desired value, the EVA would still be saturated due to the integral term, and this saturation also leads to huge overshoot and settling time. Thus, the design for avoiding this phenomenon, the so-called 'integrator winding', is another important consideration. The approach used in this study is the so-called 'integration clamping' method. It can be seen in Fig.4 that, by switching off the integration process, the controller turns into a PD control which ensures that value of the control signal would not constantly increase while the system is saturated. When the vibration amplitude reaches a predefined value for which saturation terminates, the integral term resumes operation.

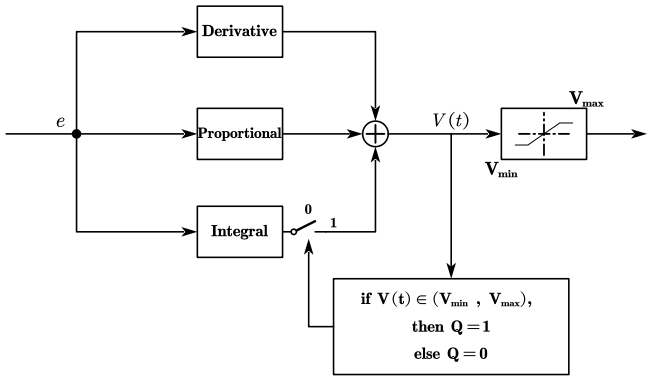


Fig.4 Schematic diagram of the anti-windup PID controller

*B. Virtual spring stiffness control methodology*

The amplitude of vibration at any point of the cable can be significantly attenuated after finding optimum parameters of PID. This approach, however, is applicable after calibrations, which requires from the field engineer a better understanding of the physical design of the EVA and a deep knowledge about classical control theory. These conditions increase complexity and cost. Therefore, an alternative control methodology is proposed that would be easily implemented and that is less complicated.

It is worth investigating the dynamics of the conventional vibration absorber before discussing the controller design. After reviewing the vibration absorber techniques, one may deem that the mass and spring stiffness of VA have decisive effects on vibration attenuation. It may therefore be tentatively concluded that the control force is obtained from these parameters. The governing equations of the cable-EVA system can be rewritten in the form

$$\begin{aligned} m_1\ddot{x}_1 + c_1\dot{x}_1 + k_1 x_1 - F_c &= F(t) \\ m_2\ddot{x}_2 + F_c &= 0 \end{aligned} \tag{14}$$

with control force $F_c = c_2(\dot{x}_2 - \dot{x}_1) + k_v(x_2 - x_1)$; and the wind induced force $F(t)$ can be expressed in the form of $A\sin\omega t$; where $\omega$ is the vibration frequency of the iced-cable and $A$ is the vibration amplitude. It is apparent by inspection of Equation (14) that only the terms $k_v(x_2 - x_1)$ and $c_2(\dot{x}_2 - \dot{x}_1)$ are related to the value of control force. As it was stated formerly, the vibration amplitude of the primary system can be eliminated when the natural frequency of the VA is tuned to the excitation frequency [15]. Consequently, the control force of the EVA system is obtained by determining the virtual spring stiffness $k_v$ from $k_v = m_2\omega^2$. Note that the damping term was predefined based on applications. For the displacement $x_2$ of the EVA, this was achieved by solving Eq.(15). Therefore, the measurement of cable vibration angular frequency $\omega$ is the key for determining the control force. In the present study, the acceleration is considered as a set of discrete signals which is

collected by the accelerometer. Applying Discrete Fourier Transform (DFT), a number of frequency components, which include the excitation frequency, are obtained as shown below:

$$X_n = \frac{1}{N}\sum_{0}^{N-1} S_p \exp(-2\pi np/N) \qquad (15)$$
$$n \in [0, N-1] \ , \ p \in [0, N-1]$$

By using a DFT-based frequency measurement method, it is possible to determine multiple frequency components of cable vibration, what enables the EVA system to be valid for more than one harmonic excitation signal. As a consequence of this consideration, the governing equation of this system can be expressed as follows

$$\begin{aligned} &m_1\ddot{x}_1 + c_1\dot{x}_1 + k_1 x_1 - F_c = A_1 \sin\omega_1 t + A_2 \sin\omega_2 t \\ &m_3\ddot{x}_3 + F_{c1} = 0 \\ &m_4\ddot{x}_4 + F_{c2} = 0 \end{aligned} \qquad (16)$$

where

$F_c = F_{c1} + F_{c2} = c_3(\dot{x}_3 - \dot{x}_1) + k_{v1}(x_3 - x_1) + c_4(\dot{x}_4 - \dot{x}_1) + k_{v2}(x_4 - x_1)$, and $m_2 = m_3 + m_4$. It follows from Eq.(16) that the control force can be determined by calculating the virtual spring stiffness $k_{v1}$ and $k_{v2}$. As stated earlier in this section, it is possible to obtain the virtual spring stiffness $k_{v1}$ and $k_{v2}$ by using the value of measured frequency from DFT in conjunction with the defined value of absorber mass.

The application of both control strategies is verified by simulations, which will be discussed in Section IV.

## IV. Simulation results

In this study, numerical simulations on a lab-scale test cable were carried out for various values of cable and ice parameters and wind induced force by using SIMULINK software. The span length of the cable was 18 m, the cross section of cable was 1.2566e-05 $m^2$, whereas the Young modulus of ice was 6.2e10 Pa [13]. The EVA system was placed 1m from the fixed end of the cable, which was recognized as the optimal operation position [16]. As a result of this consideration, the relevant parameters were calculated by using Eqs (4)-(8) and shown in Table 1. It should be noted that the damping values used in this study were calculated from the structural damping of the cable.

TABLE I. Cable and ice parameters

| Parameters | Circular ice shape | D-shape ice |
|---|---|---|
| Diameter of bare cable (m) | 4e-03 | 4e-03 |
| Cross section (m2) | 3.7699e-05 | 1.8850e-05 |
| Ice thickness (m) | 2e-03 | 2e-03 |
| Mass of iced cable (kg) | 0.1319 | 0.115 |
| Stiffness of cable (N/m) | 120.96 | 105.84 |
| Damping of cable (Ns/m) | 16.2731 | 13.025 |

Fig.5 presents the displacement response over a period of time at the position where the control is applied, before and after implementing EVA system using PID-based control method. The blue dashed line shows the results without control, the red curve represents the results under a passive VA control for the same excitation force, and the time response at the defined point of the iced cable when the EVA system is activated is depicted by the green curve.

Fig.5 (a) and (b) show that the vibration amplitude under the EVA system control are suppressed significantly for both of the lower frequency (8Hz) and higher frequency (90Hz) excitation as compared to the conventional VA. From Fig.5 (a) and (d), it can be seen that, the overshoot occurs at 0.3 s for the conventional VA system, and the motion is attenuated after about 2 s, which means a much slower response than that obtained by the EVA system. When the excitation frequency was set to 90Hz, as shown in Fig.5 (b) and (e), the amplitudes obtained with using the conventional VA are almost the same as those without control. However, when the EVA was used, the vibration amplitudes of the cable for the high excitation frequency are significantly attenuated to 0.4 mm which is 1% of that obtained with the VA.

For applications where the lift force due to wind is rapidly varied, the multiple natural frequencies of cable might be excited at the same time, what is the so-called 'beating effect'. This means that more than one frequency is present during one period of vibration. In order to examine the applicability of the proposed control for this case, a random multi-frequency excitation signal was created in accordance with the previous literature [17, 18]. The analytical function of the first imposed wind induced force is defined as $6\sin(2\pi 8) + 4\sin(2\pi 60)$. When this force acts on the iced cable, the amplitude of cable vibration dramatically increases, i.e. it is in the range of 8 mm without activating the control, as shown in Fig.5 (c). Both the conventional VA and EVA demonstrates great performance in reducing vibration amplitude. However, the response time and error are smaller with the EVA system than with the VA in vibration control. The second imposed wind induced force also consists of two frequency components and is expressed as: $7\sin(2\pi 13) + 10\sin(2\pi 50)$. In this case, it was found that, using the conventional VA, the amplitude was reduced to 3 mm as shown in Fig.5 (f). The EVA system with the use of PID control strategy gave errors (i.e. displacements) that are well within ±0.002% which is very promising in the anti-aeolian vibration applications.

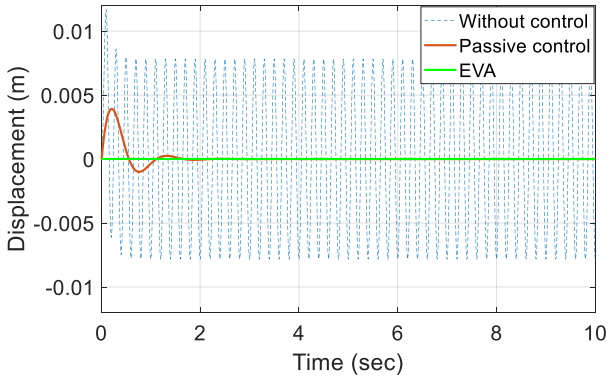


(a)

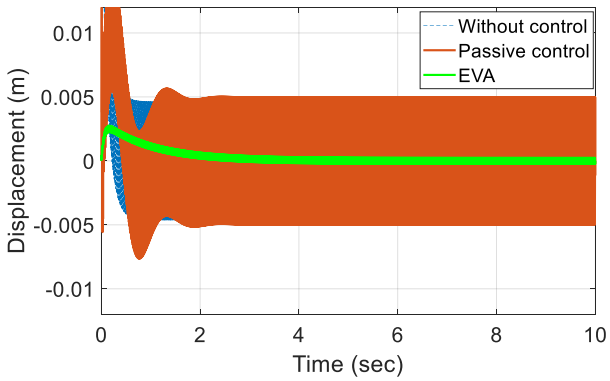


(b)

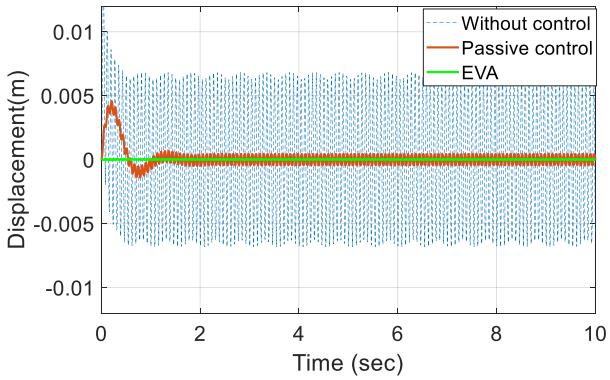


(c)

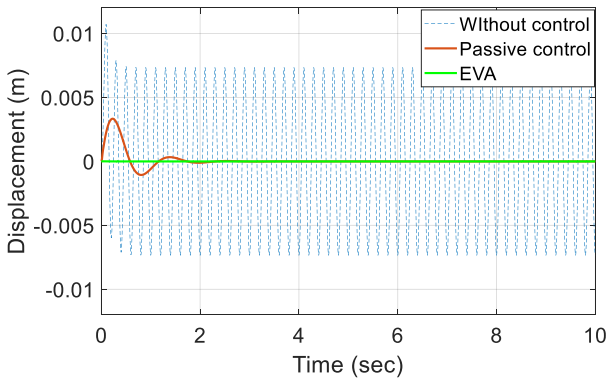


(d)

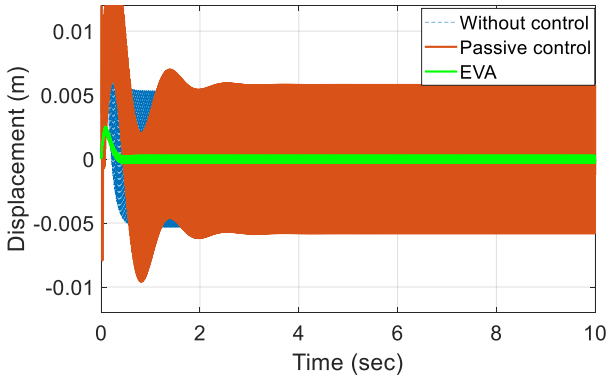


(e)

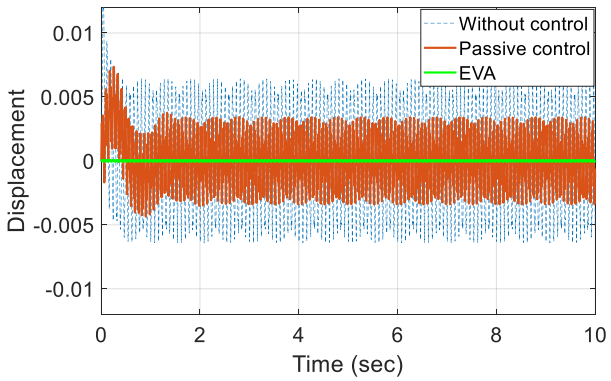


(f)

Fig.5 Time response of the iced-cable system (a)(d) comparison results for ω=16π rad/s, (b)(e) comparison results for ω=180π rad/s. (c)(f) comparison results for ω=16π and 120π rad/s. Left side (a-c): circular ice shape. Right side (d-f): D-shape ice

The virtual stiffness-based control methodology (see Section III.B) was also implemented for iced cable vibration simulations. Two different scenarios were simulated for verifying the performance of the EVA system. The first simulation was conducted as follows. Firstly, the initial frequency of the wind induced force was set to 90 Hz, and then the frequency of this wind induced force was changed to 50 Hz after 50 s. The wind induced force was then further reduced to 8 Hz after another 50 s. Once the input force sequence was imposed, the vibration control procedure was started. In the beginning of the process, Eq. (15) had to be applied to determine the DFT components of the vibration amplitude of the iced cable. After that, the frequency components were estimated, which was used to continuously calculate a control force. From Fig.6 (c), it can be seen that the estimated frequencies and the corresponding time domains are the same as the set-up values. Fig.6 (a) and (b) show the system response over 150 s. It can be seen that the vibration amplitude decreased to about 8% of its initial value at about 12 s and dropped even more until the input force was changed. When the frequency of the input force was sharply decreased to 50 Hz, an interesting behaviour might be observed. The vibration amplitude dramatically increased up to 20 mm and then started to decrease. Similar behaviour also occurs at 100 s where the input force changed again. It is worth noting that there are 1000 data points used for DFT analysis, which led to time delay following the change in the frequency. This may

have an influence on the behaviour and could possibly explain this phenomenon.

A further set of simulations was performed using the wind induced force with multiple frequencies to verify the accuracy of the control method based on virtual spring stiffness. It can be seen in Fig.6(f) that, after applying the DFT to the displacement measurement, the primary system consisted of two frequency components, which are 50 Hz and 13 Hz. The comparison of cable displacements for the cases of without control and with the virtual stiffness control for two ice shapes are shown in Fig.6(d) and (e). It was found that the virtual stiffness control method can attenuate cable vibration effectively when the 'beating effect' occurred. Comparing Fig.5 (c)(f) with Fig. 6 (d)(e) shows that the displacement response with the use of the PID-based control has much shorter settling time than the results obtained using the virtual stiffness method. This result is probably the consequence of that the frequency estimation process involves time delay in the calculation of the control force, and time delay was neglected in the PID control. This problem may be solved by using more efficient frequency estimation algorithms.

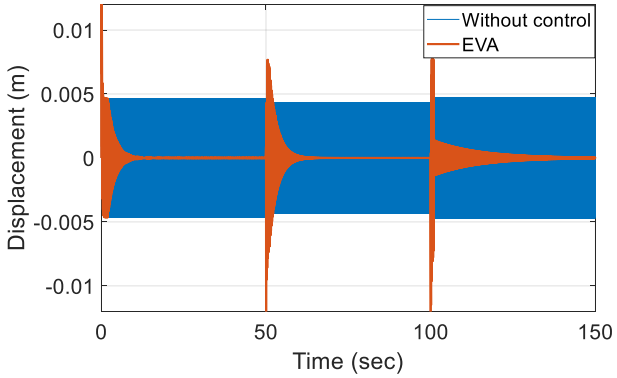


(a)

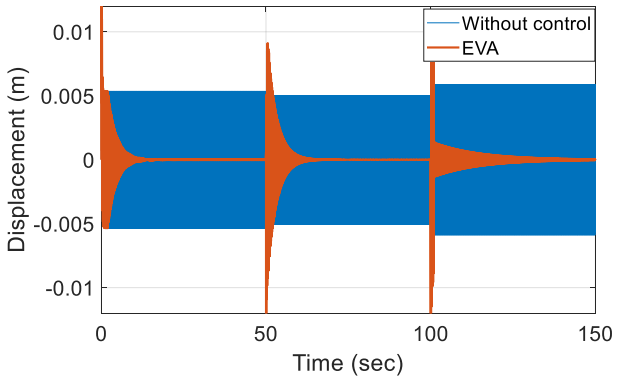


(b)

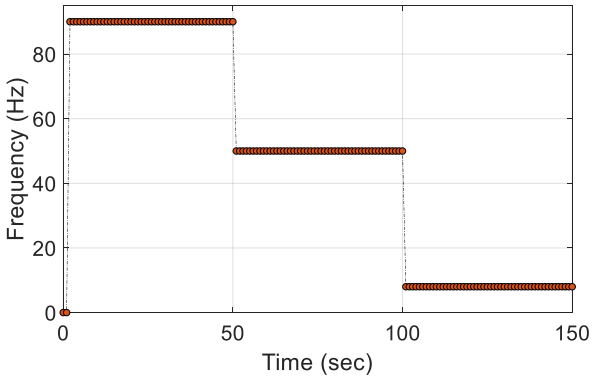


(c)

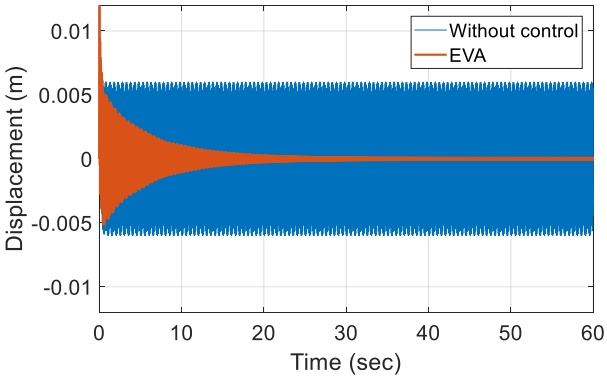


(d)

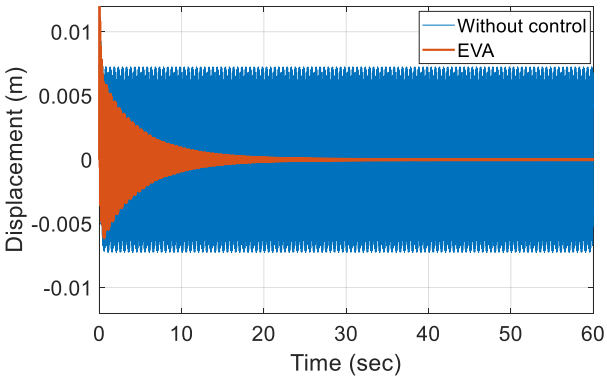


(e)

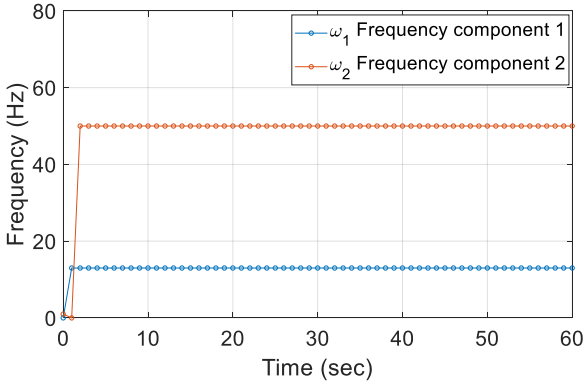


(f)

Fig.6 Simulation results for the use of virtual spring stiffness control method (a) (d) response of iced cable system (circular ice shape) (b)(e) response of iced cable system (D-shape) (c)(f) frequency measurements in Hz

## V. CONCLUSIONS

This paper describes a new hung-on vibration control technique applying an EVA system for reducing the amplitude of aeolian vibration of suspended cables in cold climate. The EVA system was designed based on active vibration control, which was able to absorb vibration energy in any position of the cable. In this study, two control methodologies, namely PID and virtual stiffness, were employed. A series of simulations were carried out to understand the performance of the EVA system with the use of two control strategies. It was observed that, with the use of PID-based control system, the cable vibration amplitude was significantly reduced, to approximately 2-3% of the amplitude obtained without any control. Moreover, the EVA system with the use of PID control method also demonstrated a promising ability to attenuate cable displacement when the 'beating phenomenon' appeared. The second control method, the virtual stiffness method, was proposed in this paper which enables the EVA system to operate without complex calibration procedures. The virtual stiffness control method exhibited remarkable performance for reducing the displacement in a relatively large excitation frequency range. The EVA system with the use of virtual stiffness method can reduce the vibration amplitude by 90% compared to the case without control. However, when the frequency suddenly changed, there was a sharp rise in cable displacement. This behaviour may be the consequence of time delay in the control force. The present paper mainly focused on developing the EVA system based on numerical simulations. Experimental study will also be considered in future research.

## ACKNOWLEDGMENT

This paper was supported by the János Bolyai Research Scholarship of the Hungarian Academy of Sciences. The research was carried out in the frame of the project "EFOP-3.6.1-16-2016-00018 – Improving the role of research + development + innovation in the higher education through institutional developments assisting intelligent specialization in Sopron and Szombathely".

## REFERENCES

[1] Fujino, Y., K. Kimura, and H. Tanaka, Wind resistant design of bridges in Japan: Developments and practices. 2012: Springer Science & Business Media.

[2] Cigada, A., et al., Vortex shedding and wake-induced vibrations in single and bundle cables. Journal of Wind Engineering and Industrial Aerodynamics, 1997. 72: p. 253-263.

[3] Farzaneh, M., Atmospheric icing of power networks. 2008: Springer Science & Business Media.

[4] Electric Power Research Institute，Transmission line reference book: wind-induced conductor motion. 1979.

[5] Speight, J.W., Conductor Vibration-Theory of Torsional Dampers. Transactions of the American Institute of Electrical Engineers, 1941. 60(10): p. 907-911.

[6] Wagner, H., et al., Dynamics of Stockbridge dampers. Journal of Sound and vibration, 1973. 30(2): p. 207-IN2.

[7] Chen, Z., et al., MR damping system for mitigating wind-rain induced vibration on Dongting Lake Cable-Stayed Bridge. Wind & structures, 2004. 7(5): p. 293-304.

[8] Jung, H.-J., B.F. Spencer Jr, and I.-W. Lee, Control of seismically excited cable-stayed bridge employing magnetorheological fluid dampers. Journal of Structural Engineering, 2003. 129(7): p. 873-883.

[9] Christenson, R.E., B. Spencer Jr, and E.A. Johnson, Experimental verification of smart cable damping. Journal of Engineering Mechanics, 2006. 132(3): p. 268-278.

[10] Ni, Y., et al., Neuro-control of cable vibration using semi-active magneto-rheological dampers. Engineering Structures, 2002. 24(3): p. 295-307.

[11] Duan, Y., Y. Ni, and J. Ko, Cable vibration control using magneto-rheological (MR) dampers, in Electrorheological Fluids and Magnetorheological Suspensions (ERMR 2004). 2005, World Scientific. p. 829-835.

[12] Wu, W. and C. Cai, Experimental study of magnetorheological dampers and application to cable vibration control. Journal of Vibration and Control, 2006. 12(1): p. 67-82.

[13] Kollár, L.E. and M. Farzaneh, Modeling the dynamic effects of ice shedding on spacer dampers. Cold Regions Science and Technology, 2009. 57(2-3): p. 91-98.

[14] Irvine, H., Cable Structures The MIT Press. Cambridge, MA, 1981: p. 15-24.

[15] Kelly, S.G., Mechanical vibrations: theory and applications. 2012: Cengage learning.

[16] Sun, L., Study on performance of damper on overhead transimission line & the precise calculation of its installation point, in Science and Physics 2003, Hefei University of technology: CNKI. p. 73.

[17] Brika, D. and A. Laneville, An experimental study of the aeolian vibrations of a flexible circular cylinder at different incidences. Journal of Fluids and Structures, 1995. 9(4): p. 371-391.

[18] Brika, D. and A. Laneville, A laboratory investigation of the aeolian power imparted to a conductor using a flexible circular cylinder. IEEE Transactions on power delivery, 1996. 11(2): p. 1145-1152.